Transactions of the 15th International Conference on
Structural Mechanics in Reactor Technology (SMiRT-15)
Seoul, Korea, August 15-20, 1999

Thermal and Mechanical Behavior of Metal Layer in Reactor Vessel Lower Head

J. S. Cho[1], K. Y. Suh[1], C. H. Chung[1], R. J. Park[2] and S. B. Kim[2]

1) Seoul National University, Korea
2) Korea Atomic Energy Research Institute, Korea

ABSTRACT

Understanding of the heat transfer and solidification processes in the molten debris pool is of fundamental importance in predicting the reactor vessel failure progression. The relocated debris pool may be stratified into layers of a debris pool and water coolant. In this connection, experiments on the heat transfer and solidification of the molten metal pool with overlying coolant with boiling were performed. The metal pool is heated from the bottom surface and the coolant is injected onto the molten metal pool. Tests were conducted by changing the bottom surface boundary condition of the metal layer and the coolant injection rate. In this study, the relationship between the Nusselt number and Rayleigh number in the molten metal pool was empirically determined. The natural convection heat transfer rates in the molten metal pool of this work are higher than the results obtained from the natural convection experiment with crust formation by subcooled coolant above and the literature correlations related with liquid metal in pure natural convection without crust formation. These enhanced heat transfer phenomena increase the cooling rate of the molten debris pool and decrease the temperature elevation and subsequent likelihood of thermomechanical failure of the reactor vessel.

I. INTRODUCTION

Molten debris coolability after a reactor accident involving core meltdown and vessel failure is currently one of the major unresolved safety issues. During a hypothetical severe accident in nuclear power plants, a significant amount of core material can melt and possibly form stratified fluid layers [1]. When two nearly immiscible liquids are brought into intimate contact, the temperature of one of the liquids may be well above the normal boiling point of the second liquid. These layers may be composed of high temperature molten debris pool and water coolant in the lower plenum of the reactor vessel [2-5] or in the reactor cavity [6]. Tbe debris pool is heated internally at decay power levels, and natural convection is the main heat transfer mechanism from the debris pool to the surroundings in the molten phase. Also, molten debris pool may be stratified into a metal layer and an oxide layer on account of their density difference [2-6]. As a result, a crust, which is a solidified layer of the molten pool, may form at the top [7,8]. Heat transfer is accomplished by a conjugate mechanism of natural convection of the molten debris pool, conduction through the solidified layer and convective boiling heat transfer to the coolant.

These complex heat transfer mechanisms between the molten debris pool and coolant layers are very important in the coolability evaluation of the molten debris pool. If a debris layer is cooled at the upper region of the molten debris pool by boiling coolant which is injected onto the molten debris pool, it is considered that the natural convection heat transfer in the molten debris pool is enhanced because the boiling heat transfer in coolant layer is very rapid.

A number of experimental and theoretical investigations were carried out to understand the solidification and the change of heat transfer rate of the debris pool, which greatly affects the accident progression. But until recently no data have been reported for heat transfer from an internally heated molten debris pool to an overlying pool of boiling coolant. Also, the detailed heat transfer mechanisms between the molten metal pool and coolant layer, in which the molten metal accompanies the solidification by coolant and the coolant goes through boiling, have not been clearly understood yet. Therefore there is a need to study the heat transfer phenomena of the molten metal pool with solidification by the boiling coolant.

Experimental studies were performed to investigate the crust formation and heat transfer characteristics of the molten metal pool with overlying coolant with boiling. Tests were conducted under the condition of the bottom surface heating in the test section and the forced convection of the coolant being injected onto the molten metal pool.

In this study, the relationship between the Nusselt number and Rayleigh number in the molten metal pool region was correlated and compared with the crust formation experiment with subcooled coolant, and other correlations available in the literature.

II. EXPERIMENTAL APPARATUS AND TEST PROCEDURE

To investigate heat transfer characteristics of the molten metal pool being solidified by the boiling coolant, the experimental apparatus was constructed as described below. The inner dimension of the rectangular test section was 25cm in length, 35cm in height, and 25cm in depth. Figure 1 shows the schematic diagram of the test apparatus. The test section is made of 10mm thick STS304 stainless steel. The heights of the molten metal and the coolant layer are 20cm and 15cm, respectively. A 20kW heater is installed in the bottom horizontal plate of the test section. The viewports are installed using a quartz glass at the front and at the back of the test section. Four sides of the test section are insulated with a 4cm thick Fiberfrax material to minimize heat loss. A digital pump is installed to deliver uniform mass flow of the coolant onto the molten metal pool. The melting pot is equipped with an 8 kW heater to melt the metal. The temperature distribution inside the test section is measured using 85 thermocouples, which are placed in five vertical arrays of thermocouple bundles located at the one-fourth, one-half and three-fourth positions of the length and width of the test section. The thermocouple is of T-type(copper-constantan) and the thermocouple bundle is made of STS304 stainless steel. Seventeen thermocouples are aligned along the vertical direction in a bundle. Fifteen of the seventeen thermocouples are immersed into the metal layer and two thermocouples are located in the coolant layer.

The simulant molten pool material is tin (Sn) with the melting temperature of 232°C. The solidification shrinkage of tin is estimated to be 2.7 % of volume [9]. For the water coolant, the input power to the bottom heating surface is varied from 6 to 14kW. The injection coolant mass flow rate is set equal to 1.0 liter/min and 2.0 liter/min in this case. For the R113 coolant, the input power is varied from 8 to 12kW and the coolant flow rate is set equal to 3.0 liter/min. The tests were performed at atmospheric pressure.

First, the metal is molten in the melting pot and injected into the test section. The metal is maintained as liquid in the test section whose bottom surface is electrically heated. To avoid any potential steam explosion when the coolant is injected onto the metal pool, the coolant is heated near to the boiling point. Next, the coolant is injected onto the molten metal in the test section at the preset mass flow rate. Then, the upper region of the molten metal layer starts to solidify and the solidified layer thickens with the lapse of time. The boiling coolant is transported to the quench tank from the test section. The vapor is condensed in the quench tank and transported to the coolant supply tank. The coolant is recirculated in a closed loop until a steady-state condition is achieved. A steady state condition is assumed when the crust thickness of the metal layer stabilizes with time. After the steady state is accomplished, the PC data acquisition system records the temperature data of the metal and coolant layers.

III. RESULTS AND DISCUSSION

The results obtained for temperature distribution in the metal layer and coolant layer are shown in Figures 2 and 3. Figure 2 shows the temperature distribution of the test section as a function of the heater input power at a water injection flow rate of 2.0 liter/min. For the case of water coolant, virtually no distinction can be made between the coolant flow rate of 1.0 liter/min and 2.0 liter/min. The portion below the horizontal dotted line is the metal layer, and the upper portion is the coolant layer. The vertical dotted line is the melting temperature of tin. The temperature varies linearly in the solidified region, and is practically uniform in the molten pool and in the coolant. Figure 3 displays the temperature profile in the metal and coolant layers for R113 with the coolant injection rate of 3.0 liter/min. The temperatures in the coolant region reveal the data at 55 ~ 57°C because the test section was pressurized to 1.3 ~ 1.4 bar due to vaporization of R113 at a rate exceeding condensation capacity of the quench tank.

Table I presents the heat transfer rates and crust thickness in the molten metal layer. The crust thickness is determined by the linear interpolation method from the thermocouple reading data and the melting temperature for tin. The heat flux can be derived from the temperature difference between the top surface and the bottom surface of the crust layer per the heat conduction equation.

The relationship between the Nusselt number and the Rayleigh number in the molten metal pool region was determined and compared against the experiment without coolant boiling and the literature correlations. The experiment without coolant boiling was performed using the low temperature melting alloy with the melting temperature of 70°C [10]. Figure 4 compares the present experimental results with the experiment without coolant boiling and other correlations in the molten metal pool region. Available correlations are the Globe and Dropkin correlation [11] for mercury, and the Park et al. correlation [12] for Wood's metal, which were obtained from an enclosure without phase changes.

Globe and Dropkin : $Nu = 0.051\, Ra^{0.333}$ $(1.51\text{x}10^5 < \text{Ra} < 6.76\text{x}10^8)$ (1)

Park et al. : $Nu = 0.092\, Ra^{0.302}$ $(2.0\text{x}10^4 < \text{Ra} < 5.0\text{x}10^7)$ (2)

The present experimental results for heat transfer from the molten metal pool are apparently higher than those without coolant boiling and other correlations. Also, test results of water coolant for heat transfer are shown to be higher than those for R113 coolant case. This difference results from the higher nucleate boiling heat transfer rate of water than of R113. It is presumed that the external cooling mechanism affects the natural convection heat transfer in the molten pool. These enhanced heat transfer phenomena increase the cooling rate of the molten debris pool and decrease the temperature elevation of the reactor vessel.

The overlying metal layer thermally attacking the reactor pressure vessel wall is considered because of the sideward heat transfer between the bulk metal layer and the reactor pressure vessel wall interface as schematically shown in Figure 5. In the figure, the sideward heat flux Q_{atk}^{ss-rv} is determined based on the maximum downward heat flux $Q_{t,rv}^{pr-vt,ms}$ from the debris oxidic pool to the lower crust plus the decay heat generation from the debris particle bed submerged in the metal layer [3]. The δ_{rv} is the reactor vessel wall thickness, the $\delta_{max,cond}$ is the maximum conduction thickness and the $\delta_{min,hoop}$ is the minimum wall thickness to support the hoop stress. The following steps are used to determine the sideward heat flux from the metal layer [3]. First, the maximum downward heat flux from the debris oxidic pool to lower crust is determined as q''_{max}. Then, the effective ΔT causing the sideward convective heat transfer from the metal layer to the vessel wall is determined as

$$\Delta T_{eff} = \min\left[188\left(\frac{q''_{max}}{106}\right)^{0.75}, \max\left(0, T_{ss} - T_{lh,i}\right)\right] \tag{3}$$

where T_{ss} is the metal layer average temperature, and $T_{lh,i}$ is the wall surface temperature in contact with the metal layer. Likewise, the effective sideward heat transfer coefficient is given by

$$h_s = 5324\left(\frac{q''_{max}}{106}\right)^{0.25} \tag{4}$$

Finally, the actual sideward heat flux is given by

$$q''_s = \min\left(1.0, \frac{t_{ss}}{t_{wall}}\right)\frac{h_s \Delta T_{eff}}{2} \tag{5}$$

where t_{ss} is the metal layer thickness and t_{wall} is the wall thickness.

If the heat flux to the wall is supplied by the solidified metal layer, the rate of crust growth is influenced by the rate of temperature rise for the steel wall as determined by the respective heat fluxes into and out of the wall. Since the escalation of the steel wall temperature would also cause the average temperature in the crust to increase, the change in the temperature must also be included as part of the effective thermal inertia for the steel wall. Also, large temperature changes in the solidified metal layer give rise to thermal

expansion. Also, the region of reactor pressure vessel contacting with the solidified metal layer has large temperature changes. The thermal expansion coefficient for SA533B1 which is used as a reactor pressure vessel material was empirically fitted by Reddy and Ayres [13]. The equation for the thermal expansion coefficient is

$$\alpha = -5.352 + 0.7320T^{0.5} + \frac{63.28}{T} \quad (\mu m/m/^{o}C) \tag{6}$$

The reactor pressure vessel wall starts to lose its strength at 800K. The yield strength versus temperature in the pressure vessel is given by Dupas and Schneiter [14].

$$\sigma_y(T) = (a_1 T + b_1)\left(\frac{\pi}{2} - \arctan\left(\frac{T - c_1}{d_1}\right)\right) - (a_2 T + b_2) \tag{7}$$

where a1, a2, b1, b2, c1 and d1 are obtained from the best fit curve of all the experimental results available.

Note however that this study was performed in the lower Ra number(10^6~10^8) and much lower metal layer temperature(100~300°C) regions than for the actual reactor accident condition. During a severe accident, the molten debris may reach the 10^9~10^{10} range of Ra number and the ~1000°C of temperature for the metallic layer [15].

IV. CONCLUSION

An experimental study was performed to investigate the characteristics of heat transfer and crust formation of the molten metal pool natural convection concurrent with forced convective boiling of the overlying coolant. In this experiment, the heat transfer is effected with accompanying solidification in the molten metal pool by coolant with boiling. The present experimental results for the heat transfer on the molten metal pool are apparently higher than those without coolant boiling and other correlations. This is probably because this experiment was performed in concurrence of solidification in the molten metal pool and the rapid boiling of the coolant. The comparison experimental tests were performed without coolant boiling, and the literature correlations were developed for the mercury without external cooling.

The current test results for the water coolant show higher heat transfer than for the R113 coolant. This results from higher nucleate boiling heat transfer rate of water than that of R113. It is considered that the external cooling mechanism affects the natural convection heat transfer in the molten pool. These enhanced heat transfer phenomena increase the cooling rate of the molten debris pool and decrease the temperature elevation of the reactor vessel. Further study is planned to investigate the effect of boiling coolant in the high temperature and high Rayleigh number region.

REFERENCES

1. Tolman, E. L., Kuan, P. and Broughton, J. M., "TMI-2 Accident Scenario Update," Nuclear Engineering & Design, Vol. 108, pp. 45-54, 1988

2. Suh, K. Y., "Modeling of Heat Transfer to Nuclear Steam Supply System Heat Sinks and Application to Severe Accident Sequences," Nuclear Technology, Vol. 106, pp. 274-291, June 1994
3. Suh, K. Y. and Henry, R. E., "Integral Analysis of Debris Material and Heat Transport in Reactor Vessel Lower Plenum," Nuclear Engineering & Design, Issue Dedicated to Dr. Novak Zuber, Vol. 151, No.1, pp. 203-221, November 1994
4. Suh, K. Y. and Henry, R. E., "Debris Interactions in Reactor Vessel Lower Plena During a Severe Accident: I. Predictive Model," Nuclear Engineering & Design, Vol. 166, pp. 147-163, October 1996
5. Suh, K. Y. and Henry, R. E., "Debris Interactions in Reactor Vessel Lower Plena during a Severe Accident: II. Integral Analysis," Nuclear Engineering & Design, Vol. 166, pp. 165-178, October 1996
6. Bradley, D. R. and Gardner, D. R., CORCON-MOD3 : An Integrated Computer Model for Analysis of Molten Core-Concrete Interactions, NUREG/CR-5843, 1992
7. Blose, R. E. et al., "SWISS : Sustained Heated Metallic Melt/Concrete Interactions with Overlying Water Pool," NUREG/CR-4727, 1987
8. Tarbell, W. W. et al., "Sustained Concrete Attack by Low-Temperature Fragmented Core Debris," NUREG/CR-3042, 1987
9. Boyer, H. E. et al., *Metals Handbook*, American Society for Metals, 1985
10. Park, R. J. et al., "Crust Formation and Its Effect on Heat Transfer in the Molten Metal Pool," International Meeting on Advanced Reactors Safety ARS97, pp. 81-88, Orlando, FL, USA, June 1997
11. Globe, S. and Dropkin, D., "Natural Convection Heat Transfer in Liquid Confined by Two Horizontal Plates and Heated from Below," J. of Heat Transfer, Vol. 97, pp. 24-30, 1959
12. Park, R. J. et al., "Effect of Crust Thickness Increase on Natural Convection Heat Transfer in the Metal Pool," Proceedings of the NTHAS98 : First Korea-Japan Symposium on Nuclear Thermal Hydraulics and Safety, pp. 448-455, Pusan, Korea, October 1998
13. Reddy, G. B. and Ayres, D. J., "High Temperature Elastic-Plastic and Creep Properties for SA533 Grade B Class 1 and SA508 Material," EPRI-NP-2753, 1982
14. Dupas, P. and Schneiter, J. R., "Simplified methods applied to the complete thermal and mechanical behavior of a pressure vessel during severe accident," PVP-Vol. 331, pp. 145-151, 1996
15. Theofanous, T. G. et al., In-Vessel Coolability and Retention of a Core Melt, DOE/ID-10460, July (1995)

Table I. Heat Transfer Rate and Crust Thickness of the Molten Metal Pool

Water					R113		
Input Power (kW)	Crust Thickness (cm)		Heat Flux (W/m^2)		Input Power (kW)	Crust Thickness (cm)	Heat Flux (W/m^2)
	1 liter/min	2 liter/min	1 liter/min	2 liter/min		3 liter/min	3 liter/min
6	10.67	10.91	6.91E+4	6.64E+4	8	11.36	8.87E+4
8	8.55	7.16	9.38E+4	9.52E+4	9	10.16	9.52E+4
10	5.81	5.61	1.23E+5	1.16E+5	10	8.49	1.13E+5
12	5.21	5.14	1.39E+5	1.25E+5	11	7.04	1.31E+5
14	3.10	2.90	2.15E+5	2.29E+5	12	4.60	1.86E+5

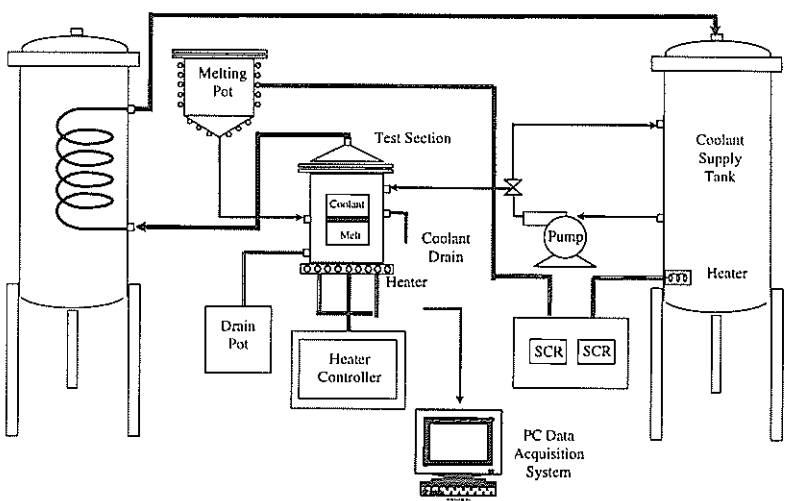

Figure 1. Schematic Diagram of the Experimental Facility

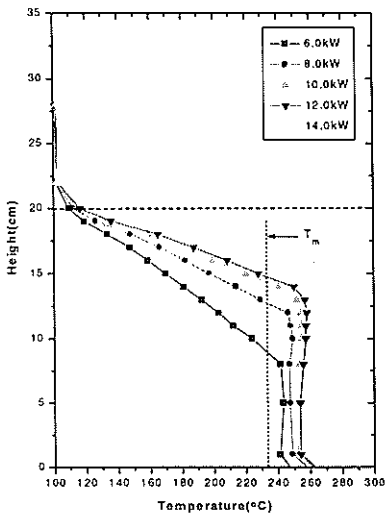

Figure 2. Temperature Distribution in Metal and Coolant Layers (Water Coolant Injection Rate : 2.0 liter/min)

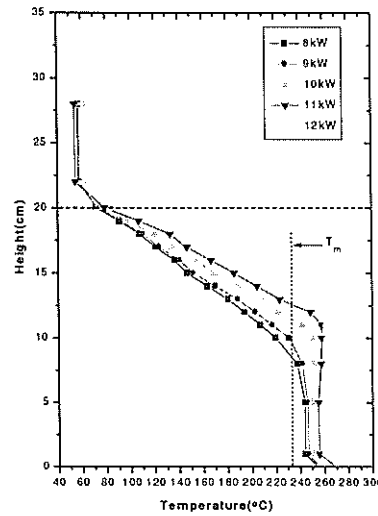

Figure 3. Temperature Distribution in Metal and Coolant Layers (R113 Coolant Injection Rate : 3.0 liter/min)

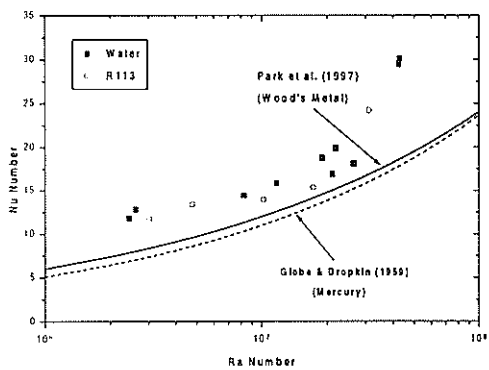

Figure 4. Comparison of the Present Results with Literature Correlations

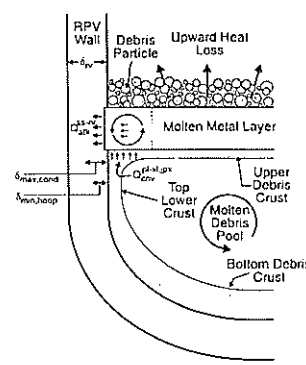

Figure 5. Metal Layer Attack on RPV Wall (Taken from Suh and Henry [3])